Amer A. Ramadhan [1]
Moahmmed M. Hameed [2]
Moahmmed O. Salman [3]
Eman M. Nasir [1]

[1] *Department of Physics, College of Science, University of Baghdad, Baghdad, IRAQ*
[2] *Ministry of Higher Education and Scientific Research, Baghdad, IRAQ*
[3] *Department of Medical Physics, College of Applied Sciences, University of Fallujah, Fallujah, IRAQ*

Enhanced Gas Sensing Performance of Plasma-Treated Tin-Zinc–Oxide Thin Films Deposited by Spray Pyrolysis

This study explores the impact of plasma treatment on the gas sensing capabilities of tin-zinc oxide (SZO) composite thin films, fabricated through spray pyrolysis. It investigates variations in Sn atomic ratios, ranging from 0.0 to 0.6. The study explores the effects of plasma etching, utilizing cold plasma induced by a plasma torch, on the morphological and electrical characteristics of the prepared SZO films. Findings, revealed by Field Emission Scanning Electron Microscopy (FE-SEM), illustrates a noteworthy porous structure with uniformly sized spherical nanoparticles. The introduction of plasma induces significant surface porosity, thereby enhancing gas sensing performance through the porous SZO layer. Testing against NO_2 gas indicates an optimum operating temperature of 150°C. These results emphasize the effectiveness of the plasma exposure method in significantly improving the efficiency of NO_2 gas sensing, marking a crucial advancement in sensor technology.

Keywords: Tin-zinc oxide; Gas sensing; Plasma treatment; Spray pyrolysis
Received: 12 February 2024; **Revised:** 05 May 2024; **Accepted:** 12 May 2024

1. Introduction

Gas sensors with high sensitivity across a wide range of gas concentrations are essential for various applications, including indoor safety and environmental monitoring [1,2]. Among the materials investigated for gas sensing applications, zinc oxide (ZnO) nanostructures have garnered considerable attention [3]. The utilization of porous thin film structures enhances their interaction with gas molecules due to their enlarged surface area, offering high sensitivity and improve selectivity to target gases. Altering porous structures in fabricated thin films through adjustments deposition parameter enhances the functionality of resulting devices [4]. Tin-zinc oxide (SnZnO) composite films possess distinct physical and chemical properties suitable for gas sensor applications, demonstrating sensitivity to various gases [5]. Spray pyrolysis stands out as a popular, cost-effective, and easily controllable technique for fabricating thin films, particularly metal oxides [6,7]. Nevertheless, defects in prepared SnZnO films may compromise gas sensing efficiency [8]. Researchers employ various post-deposition processing techniques to address these challenges and enhance sensor performance [9]. Among these techniques, plasma processing exhibits significant potential in improving gas sensing performance [10]. Plasma etching involves bombarding material surfaces with active ions, thereby altering surface structure parameters such as roughness and crystalline grain size, consequently impacting gas sensing properties [11,12].

Despite the potential benefits, limited studies have specifically investigated the effect of plasma treatment on SnZnO films synthesized via spray pyrolysis. Understanding the influence of plasma treatment on the gas sensing performance of SnZnO films is fundamental for modifying their properties to meet specific gas sensing application requirements [13]. Zinc stanate (Zn_2SnO_4) stands out as a significant ternary oxide in numerous applications [14]. Among its phases, Zn_2SnO_4 exhibits a unique crystal structure and chemical composition, be suitable for gas sensing applications, as evidenced in previous studies [15]. Zinc stanate thin films can be prepared using various techniques, including chemical vapor deposition and spray pyrolysis. Plasma treatment has the potential to modify the surface properties of the active layer for gas sensing by enhancing crystallinity, surface morphology, and gas adsorption capability [16]. In 2020, Zhang et al. investigated the doping effect of copper and iron on zinc Stanate and observed improved gas sensing performance towards specific target gases [15,17].

This paper aims to investigate the effect of plasma treatment on the gas sensing performance of SnZnO films prepared by spray pyrolysis. The changes in the structural, and morphological properties of the films after plasma etching and correlate them with the gas sensing response at different concentration ranges were investigated. This study provide a strategy for the design and optimization of gas sensing materials.

2. Experimental Part

Composite thin films of $(ZnO)_{1-x}(SnO_2)_x$ at various molar ratios were synthesized employing a spray pyrolysis technique. A 0.1 M aqueous solution comprising zinc chloride ($ZnCl_2$) and tin chloride $SnCl_2$ (sourced from Sigma-Aldrich) was prepared in distilled water using a magnetic stirrer. Prior to application, the solutions underwent filtration using filter paper. The thin films were deposited onto glass slides via spray deposition, with the substrate temperature maintained at 500°C. The spray nozzle was positioned 30cm above the substrates in a vertical configuration. Spraying was conducted at a rate of 1 mL/min using compressed air at 4 bar pressure. The thickness of the films, approximately 200nm, was determined using Angstrom TFProbe optical spectroscopic reflectometer. The crystalline structure of the prepared samples was analyzed using Shimadzu XRD-6000 X-ray Diffraction system. Surface morphology was assessed using a ZEISS Sigma field-emission scanning electron microscope.

To enhance the gas sensing properties of SZO thin films, a novel approach utilizing a plasma torch was employed. High alternating voltage operating at 10kV, and a controlled flow of argon were utilized. The deposited SZO thin films underwent plasma treatment at a distance of 2 cm from the plasma orifice for 3 minutes. The argon flow rate was adjusted to optimize the plasma treatment process to 1 SLM. This plasma treatment induced surface modifications.

The gas sensing efficiency of as-prepared and plasma-modified SZO samples was evaluated against NO_2 gas at different concentrations and operating temperatures of 50, 100, 150, and 200°C. Initially, the as-deposited samples were tested, followed by the plasma-treated samples to assess the effect of plasma etching on their performance. The change in electrical resistance was determined as the response of the fabricated gas sensors for each operating temperature within the gas concentration range of 2 to 100 ppm. The measurements were conducted in a controlled environment using a gas chamber with precise concentration control.

3. Results and Discussion

The structural properties of SZO thin films were investigated using x-ray diffraction. Figure (1) shows the diffraction patterns of SZO thin films deposited at different Sn molar ratios on glass substrates. These patterns reveal polycrystalline structures and distinctive phases depending on the Sn molar ratio for the started precursor. Specifically, when the Sn molar ratio was x=0.2, the diffraction pattern showed ZnO phase of hexagonal crystal (according to the ICDD card number 36-1451). This suggests successful incorporation of Sn atoms into the ZnO lattice without significant alteration to the host lattice structure at lower Sn ratios.

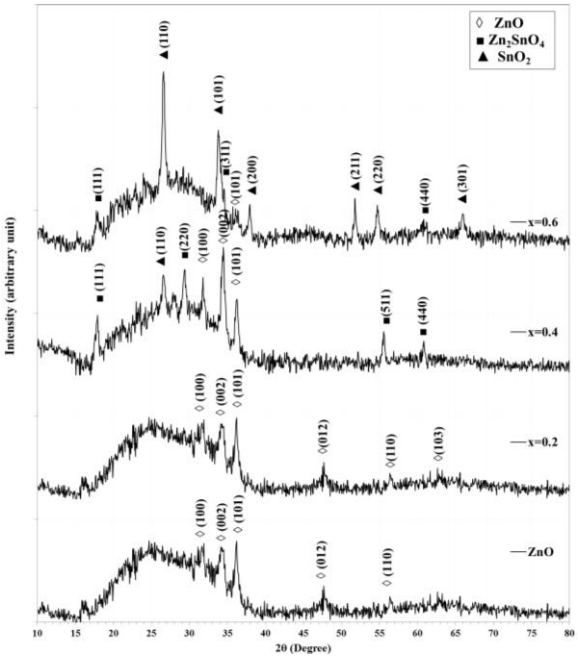

Fig. (1) XRD patterns for SZO thin films at different Sn:Zn atomic ratio

Increasing the Sn ratio to x=0.4, additional peaks corresponding to the Zn_2SnO_4 and SnO_2 phases (according to the ICDD card numbers 24-1470 and 41-1445, respectively) emerged alongside the ZnO diffraction lines. This observation aligns with the stoichiometric ratio required for the formation of Zn_2SnO_4 (Sn:Zn=1:2), indicating a complex composite structure with the coexistence of multiple phases within the thin film.

Further increase in the Sn ratio to x=0.6 led to enhanced crystallinity of the SnO_2 phase while reducing the intensity of the Zn_2SnO_4 phase. The prominent peaks of the SnO_2 phase, accompanied by smaller peaks corresponding to other phases, signify higher Sn content within the film. Consequently, the phase composition of the SZO thin film was observed to be highly influenced by the atomic ratio of Zn to Sn, with different compositions resulting in the formation of distinct phases.

These findings are consistent with previous research employing alternative techniques to achieve similar Zn:Sn ratios. For example, Kurz et al. utilized sol-gel spin coating at a Zn:Sn molar ratio of 32:68, leading to the formation of Zn_2SnO_4 [18]. Similarly, Sun et al. achieved Zn_2SnO_4 formation through solvothermal synthesis, employing a Zn:Sn molar ratio of 1:2 [19]. The reproducibility of Zn_2SnO_4 formation across different techniques and ratios supports the reliability of the observed phase composition in the SZO thin film system.

The phase diagram of the Zn-Sn-O system provides valuable insights into the composition-dependent behavior of this ternary oxide system. In order to explore the phase distribution and composition ranges within this system, a two-dimensional x-ray analysis was conducted utilizing

XPowder software, which shows the phase distribution within the Zn-Sn-O system. This analysis, as illustrated in Fig. (3), offers the point of phases variations. The dominant phase was ZnO at x=0.1. Interestingly, this phase remained predominant even at higher Sn content. This suggests that ZnO exhibits the highest stability compared to other phases within this system. At the composition range of x= 0.2 to 0.3, the XRD analysis showed the emergence of a new phase of Zn_2SnO_4. This phase, is attends within this range indicates a compositional preference for a specific zinc to tin ratio, around x=0.4. While, increasing the x ratio more than 0.4 makes the dominant phase is the SnO_2.

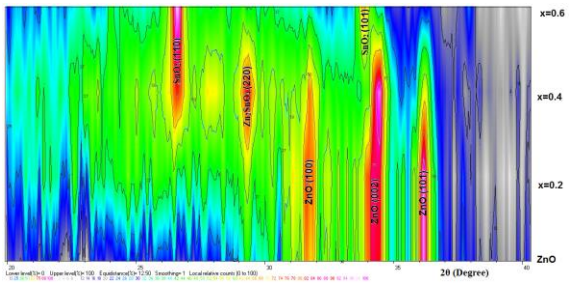

Fig. (2) 2D XRD analysis attained by XPowder software for Zn-Sn-O system with the Sn malar ratio

The FE-SEM was conducted to examine the surface morphology of the prepared thin films. Figure (3) displays morphological images of the ZnO and SZO composite thin films. The fabricated ZnO thin films constructed from spherical particles with a similar size around 100 nm diameter. These spherical nanoparticles were closely interconnected, contributing to the overall porous architecture. These characteristics are advantageous for gas sensing applications, as the performance of such sensors heavily relies on nanostructure shapes, surface-to-volume ratios, and the connectivity between adjacent nanoparticles [20]. The sample composed with 0.2 atomic ratio of Sn cause to decrease the porosity due to enhanced particle attachment. Increasing in the Sn ratio to 0.4 resulted in the presence of two distinct particle types. Larger particles appeared as Irregular rock-like shapes of diameter about 600 nm, alongside the smaller particles measuring around 100 nm, indicating the existence of two phases within the structure. Lastly, the sample prepared with 0.6 Sn ratio displayed particles of 200 nm diameter attached with nanoparticles forming whole structure. The porosity significantly reduced at this ratio.

Figure (4) shows the FE-SEM images of both ZnO and SZO composite thin films subsequent to plasma treatment. The ZnO film exhibited a uniformly distributed porous structure comprising spherical particles of approximately 100 nm in diameter. The plasma-treated samples exhibited noteworthy enhancements in porosity compared to the untreated SZO samples. The spherical nanoparticles exhibited close interconnection act as channels for electrical connection which is a significant affect the gas sensing mechanism. The alterations in surface and interfacial properties induced by plasma treatment facilitated gas adsorption, thereby leading to improved sensitivity towards target gases. Such attributes confer several advantages for gas sensing applications, as sensor performance is markedly influenced by the size and morphology of nanostructures, as well as the interconnectivity among adjacent nanoparticles [21]. The barrier height across the charge carriers within the interconnected channels is depending upon the formation of a depletion layer subsequent to electron extraction by adsorbed oxidized molecules on the sample surface. This phenomenon leads to alterations in the energy barrier across the channels relative to gas concentration. Consequently, this process effectively enhances the gas sensing performance [22].

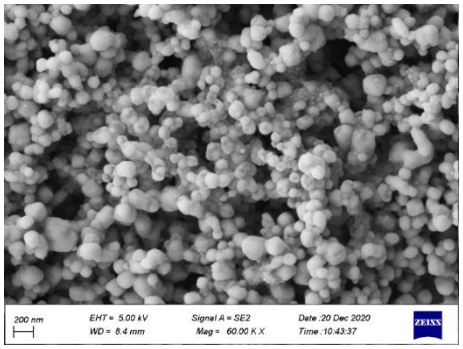

(a)

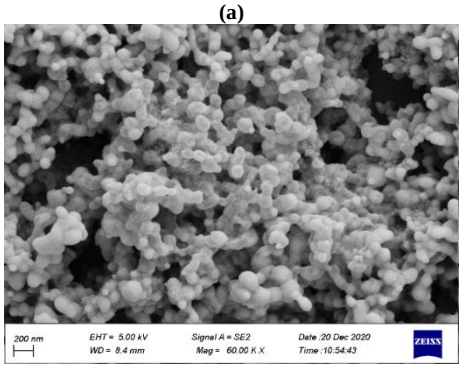

(b)

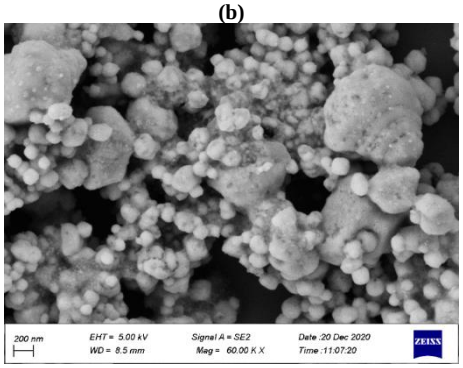

(c)

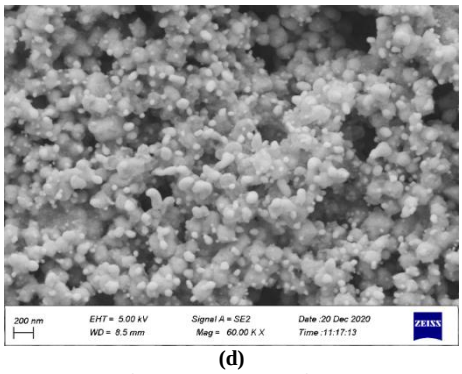

(d)

Fig. (3) Top view of FE-SEM images for ZnO layer (a) SZO composite thin films at x= 0.2 (b), x= 0.4 (c), and x=0.6 (d)

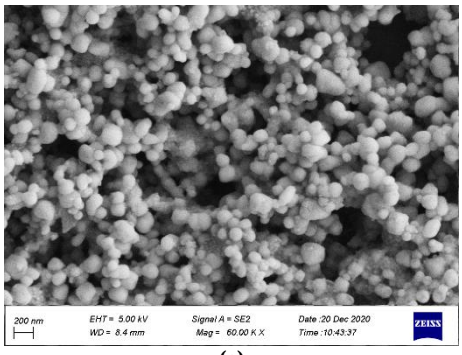

(a)

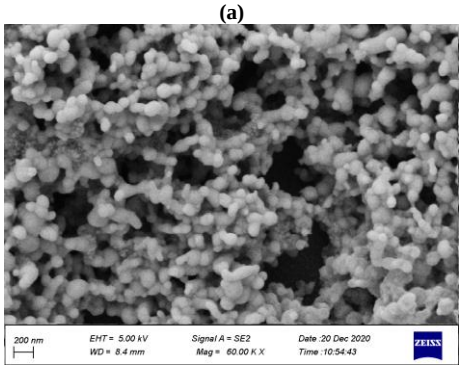

(b)

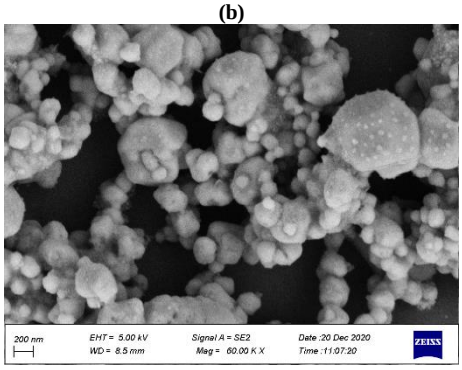

(c)

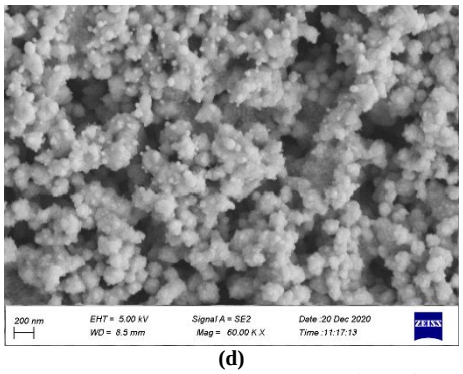

(d)

Fig. (4) The FE-SEM images for ZnO thin film after plasma treatment (a) SZO composite thin films at x=0.2 (b), x=0.4 (b), and x=0.6 (c)

Figures (5) depicts the variation of resistance for the as prepared SZO thin films, which was prepared under various tin ratio, while subjecting the samples to a 20 ppm NO_2 gas at 150°C working temperature. Across all samples, exposed to the gas resulted in an increase in resistance. This phenomenon can be explained by the extraction of a more electrons from material due to the oxidation reaction by the target gas. Gas adsorption led to a reduction in sample conductivity due to two main factors. Firstly, it caused a decrease in the charge carriers concentration, and secondly, it reduce the mobility of carriers by forming a surface depletion layer, which built a potential barrier across the charge carriers at the grain boundaries. The sensitivity various according to surface morphology, so the largest variation occurred for the x=0.2 sample. To enhance sensing behaviour, it is crucial to fine-tune the morphology of the sensing materials and establish well-defined channels of connection between the nanostructures. By optimizing these factors, gas sensing performance can be significantly improved [23].

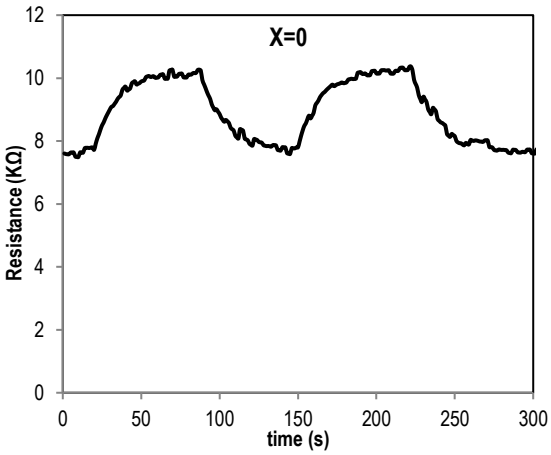

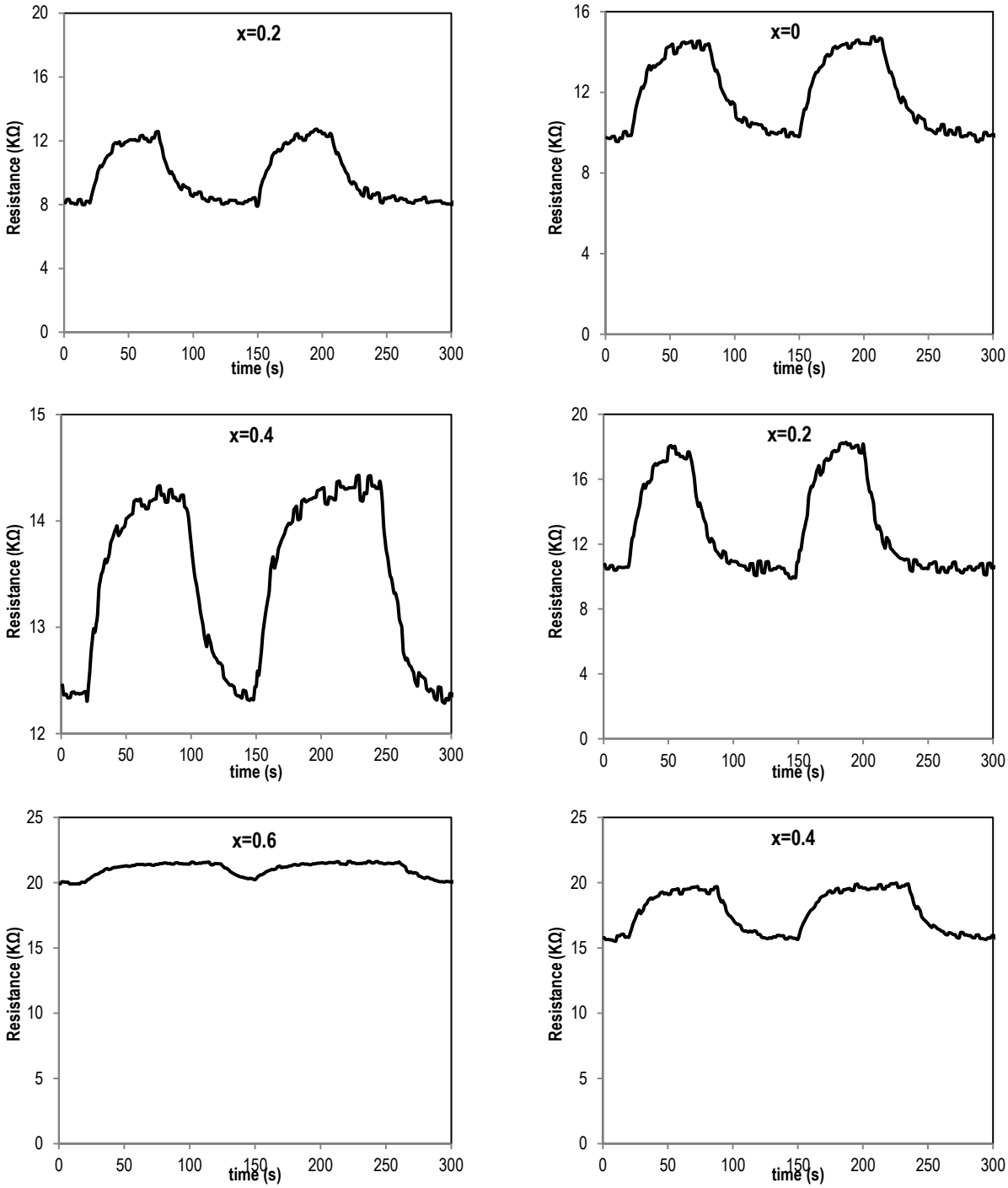

Fig. (5) Variation of resistance of the SZO-based sensor prepared at different x against 20 ppm NO_2 gas exposure at 150°C working temperature

Figures (6) displays the variation of resistance with time for sensor based on the plasma treated-SZO thin films prepared at different x against 20 ppm NO_2 gas at 150°C. The variation in resistance fluctuation improved after plasma exposure specially for the x=0.2 sample compared to the as prepared samples due to the variation in samples porosity, so increase the surface area that exposed to NO_2 gas.

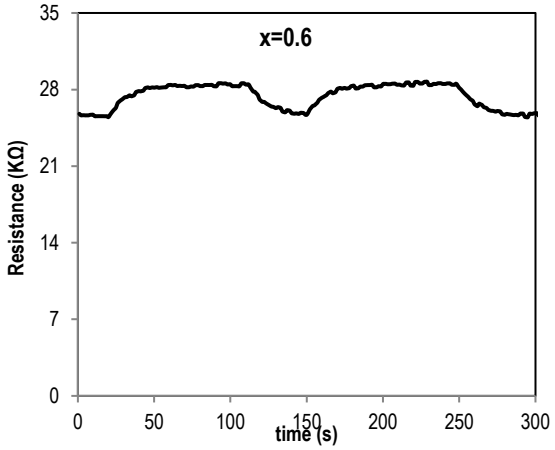

Fig. (6) Variation of resistance of the SZO-based sensor prepared at different x against 20 ppm NO_2 gas exposure at 150°C after plasma treatment

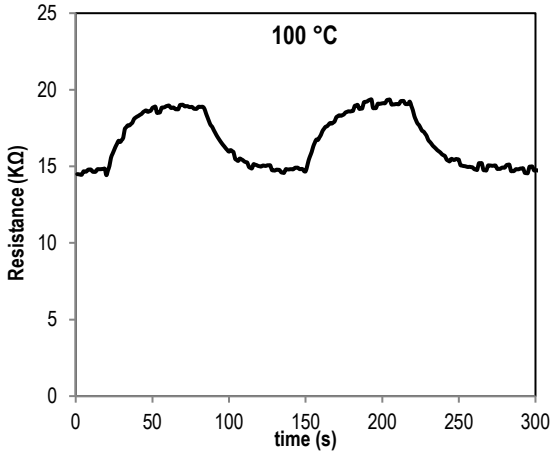

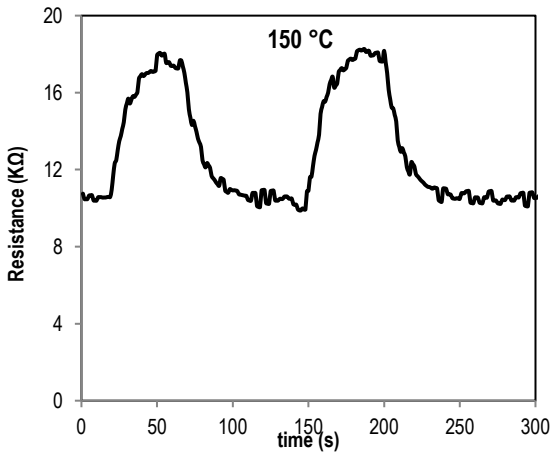

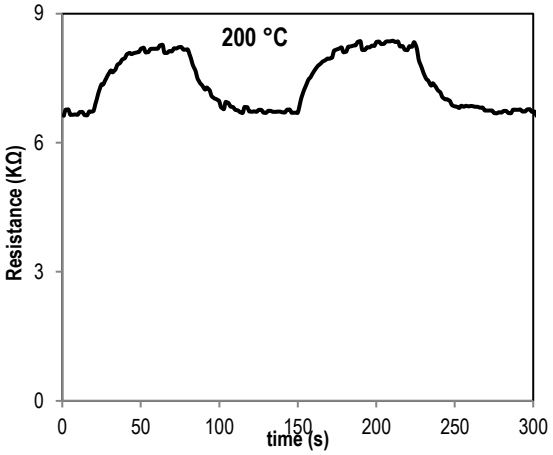

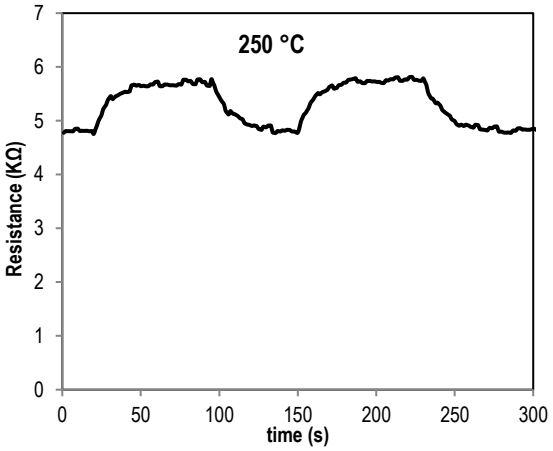

Fig. (7) Variation of resistance against 20 ppm NO_2 at different working temperatures for the SZO-based sensor at x=0.2 after plasma treatment

Figure (8a) illustrates a comparison between sensitivity before and after plasma treatment against 20 ppm NO_2 with the Sn ratio at 150°C operating temperature. The optimum sensitivity appeared for x=0.2, and the sensitivity improved after plasma treatment for all samples, but with different ratios, and the best enhancement was 1.4 folds for x=0.2. Figure (8b) illustrates the changes in gas sensitivity to 20 ppm NO_2 gas for x=0.2 following plasma treatment at different working temperatures. The highly dependence of sensitivity on the temperature due to variations in chemical response rates and gas desorption. The highest sensitivity is observed at an optimal temperature of 150°C. At lower temperatures, the sensitivity is constrained by the chemical response speed, while at higher temperatures, which is governed throughout the desorption of gas particles. A balance between these two processes is achieved at a moderate point, resulting in the sensor's optimal sensitivity value [24].

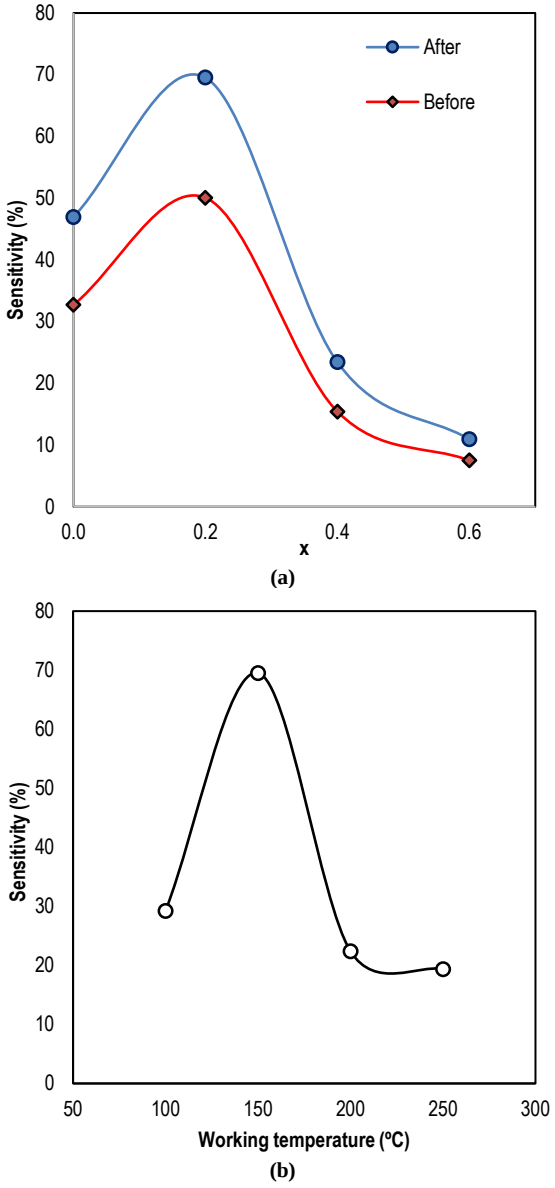

Fig. (8) Variation of sensitivity against 20 ppm NO_2 :(a) at 150°C against Sn ratio before and after plasma treatment, (b) for x=0.2 after plasma treatment with operating temperature

Figure (9) shows the sample response of sensor based on SZO with the optimum ratio of x=0.2 at 150°C against different gas concentrations. It seem that the response depend on gas concentration within the range of 5 to 40 ppm. The depletion layer thickness is influenced by the amount of adsorbed gas, resulting in an elevation of the energy barrier concerning gas concentration. Therefore, changes in sample resistance serve as an indicator of gas concentration [25].

Figure (10) shows the best exponent-curve fitting of variation of response for the SZO sample at x=0.2 after plasma treatment against the concentration of NO_2 (5-40 ppm) at 150°C operating temperature. The normalized fitting of gas sensitivity against gas concentration was $y = 0.6671x^{0.3263}$ with high fitting accuracy of R^2=0.9533.

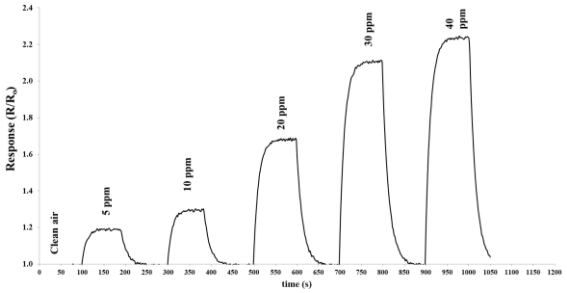

Fig. (9) The sensor response of SZO prepared at x=0.2 against different NO_2 gas concentrations at 150°C operating temperature

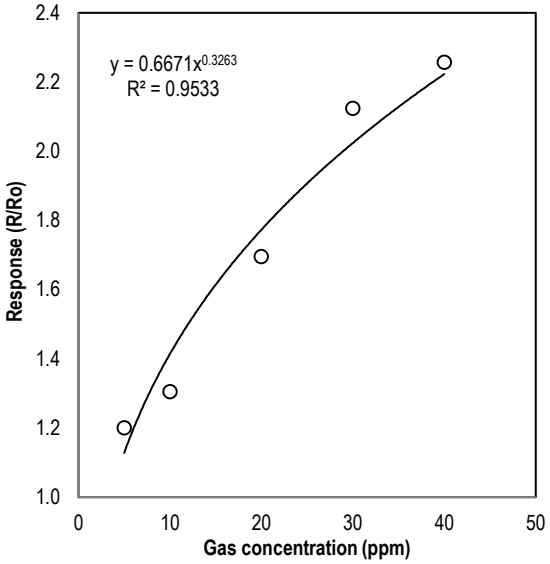

Fig. (10) The fitting of variation of response for the SZO sample at x=0.2 after plasma treatment with gas concentration at 150°C operating temperature

4. Conclusions

The investigation into composition-dependent of SZO nanocomposites thin films deposited via spray pyrolysis shows emergence of Zn_2SnO_4 at 0.4 Sn ratio. Plasma etching cause significant morphological changes in films, enhancing sensing capabilities. Improved sensitivity and response to NO_2 gas are observed across different concentrations and operating temperatures, notably peaking at 150 °C. Moreover, gas sensors based on SZO nanocomposites with x=0.4 exhibit enhanced sensitivity and response compared to others, underscoring the essential Sn ratio in determining gas sensing properties. These findings underscore the efficacy of plasma exposure in enhancing gas sensitivity of prepared SZO thin film toward NO_2 across various conditions.

References

[1] K. Anand et al., "Hydrogen sensor based on graphene/ZnO nanocomposite", *Sens. Actuat. B: Chem.*, 195 (2014) 409-415.

[2] M. Laurenti and V. Cauda, "Porous zinc oxide thin films: Synthesis approaches and applications", *Coatings*, 8(2) (2018) 67.

[3] W. Zhang et al., "Three-terminal nonvolatile memory photodetectors based on rationally

engineered heterostructured tin zinc oxide nanowires", *Curr. Appl. Phys.*, 48 (2023) 34-41.
[4] M.O. Salman, M.A. Kadhim and A.A. Khalefa, "CdO:SnO_2 Composite UV-Assisted Room Temperature Ozone Sensor", *Iraqi J. Sci.*, 64(3) (2023) 1190-1202.
[5] Z. Chen et al., "Performance improvement of tin-doped zinc oxide thin-film transistor by novel channel modulation layer of indium tin oxide/tin zinc oxide", *Jap. J. Appl. Phys.*, 54(4S) (2015) 04DF03.
[6] M. Thirumoorthi and J.T.J. Prakash, "Doping effects on physical properties of (101) oriented tin zinc oxide thin films prepared by nebulizer spray pyrolysis method", *Mater. Sci. Eng. B*, 248 (2019) 114402.
[7] P. Chesler et al., "Tin–Zinc oxide composite ceramics for selective CO sensing", *Ceram. Int.*, 42(15) (2016) 16677-16684.
[8] A. Ani et al., "Evaluation of spray pyrolysed In:ZnO nanostructures for CO gas sensing at low concentration", *J. Mater. Sci.: Mater. in Electron.*, 32(17) (2021) 22599-22616.
[9] L.H. Kathwate et al., "Ammonia gas sensing properties of Al doped ZnO thin films", *Sens. Actuat. A: Phys.*, 313 (2020) 112193.
[10] K. Hu et al., "Enhanced hydrogen gas sensing properties of Pd-doped SnO_2 nanofibres by Ar plasma treatment", *Ceram. Int.*, 46(2) (2020) 1609-1614.
[11] S. Sahoo et al., "A review on supercapacitors based on plasma enhanced chemical vapor deposited vertical graphene arrays", *J. Ener. Stor.*, 53 (2022) 105212.
[12] K. Hu et al., "Ar plasma treatment on ZnO–SnO_2 heterojunction nanofibers and its enhancement mechanism of hydrogen gas sensing", *Ceram. Int.*, 46(13) (2020) 21439-21447.
[13] S. Dabbabi et al., "Fabrication and Characterization of Sensitive Room Temperature NO_2 Gas Sensor Based on $ZnSnO_3$ Thin Film", *phys. stat. sol. (a)*, 216(16) (2019) 1900205.
[14] S. Dinesh et al., "Hydrothermal synthesis of zinc stannate (Zn_2SnO_4) nanoparticles and its application towards photocatalytic and antibacterial activity", *J. Mater. Sci.: Mater. Electron.*, 27(9) (2016) 9668-9675.
[15] Z. Lu et al., "Electrospun ZnO–SnO_2 Composite Nanofibers and Enhanced Sensing Properties to SF_6 Decomposition Byproduct H_2S", *Front. Chem.*, 6 (2018) in "Advanced Nanomaterials for Sensing Applications" Z. Wang, W. Zeng and Z. Li (ed.).
[16] A. Rovisco et al., "Microwave-Assisted Synthesis of Zn_2SnO_4 Nanostructures for Photodegradation of Rhodamine B under UV and Sunlight", *Nanomater.*, 12(12) (2022) 2119.
[17] L. Chen et al., "Regulation of intrinsic physicochemical properties of metal oxide nanomaterials for energy conversion and environmental detection applications", *J. Mater. Chem. A*, 8(34) (2020) 17326-17359.
[18] A. Kurz and M.A. Aegerter, "Novel transparent conducting sol-gel oxide coatings", *Thin Solid Films*, 516 (2008) 4513-4518.
[19] G. Sun, S. Zhang and Y. Li, "Solvothermal synthesis of Zn_2SnO_4 nanocrystals and their photocatalytic properties", *Int. J. Photoener.*, 2014 (2014) 25-29.
[20] P.H. Suman et al., "Comparative gas sensor response of SnO_2, SnO and Sn_3O_4 nanobelts to NO_2 and potential interferents", *Sens. Actuat. B: Chem.*, 208 (2015) 122-127.
[21] H. Du et al., "Investigation of gas sensing properties of SnO_2/In_2O_3 composite hetero-nanofibers treated by oxygen plasma", *Sens. Actuat. B: Chem.*, 206 (2015) 753-763.
[22] P. Feng et al., "Gas sensors based on semiconducting nanowire field-effect transistors", *Sensors*, 14(9) (2014) 17406-17429.
[23] Y.F. Sun, S.B. Liu and F.L. Meng, "Metal oxide nanostructures and their gas sensing properties: A review", *Sensors*, 12(3) (2012) 2610-2631.
[24] O.A. Fahad, H.S. Al-Jumaili and M.H. Suhail, "Studies on spray pyrolised nanostructured SnO_2 thin films for H_2 gas sensing application", *Adv. Enviro. Biol.*, 17(2) (2014) 125-141.
[25] A.A. Ramadhan, F.T. Ibrahim and E.M. Nasir, "The Preparing and Characterization of Nanocomposite (PTh/SWCNT) for NO_2 Gas Sensing", *J. Phys.: Conf. Ser.*, 1660 (2020) 012093.

